Check for updates

Investigating multigelator systems across multiple length scales†

Libby J. Marshall, [a] Simona Bianco, [a] Rebecca E. Ginesi, [a] James Doutch, [b] Emily R. Draper [a] and Dave J. Adams *[a]

Preparation of multicomponent systems provides a method for changing the properties of low molecular weight gelator (LMWG)-based systems. Here we have prepared a variety of multicomponent systems where both components are *N*-functionalised dipeptide-based LMWGs that may either co-assemble or self-sort when mixed. We exemplify how varying the concentration ratio of the two components can be used to tune the properties of the multicomponent systems pre-gelation, during gelation and in the gel state using viscosity and rheology measurements, circular dichroism, NMR and small angle neutron scattering. We also investigate the effect of changing the chirality of a single component on the properties of these systems. While predicting the outcome of multicomponent assembly is a challenge, the preparation of a variety of systems allows us to probe the factors affecting their design. This work provides insights into how the properties of multicomponent systems composed of two gelators with the same basic structural design can be tuned by varying the chirality and the concentration ratio of the two components and considering the behaviour of the two components when alone.

Introduction

Peptide-based low-molecular weight gelators (LMWGs) tend to self-assemble to form long, 1D structures in aqueous solution through the formation of directional non-covalent interactions such as hydrogen bonds and π–π stacking interactions (Fig. 1).[1–3] Most examples of gels formed using such LMWGs use a single molecule that assembles to give a network. However, there are many possibilities and opportunities when using multicomponent systems. Mixing two LMWGs in aqueous solution results in a range of possible outcomes in both the solution and gel states, with some of the possible outcomes exemplified in Fig. 1. The two gelators may prefer to interact only with themselves, resulting in self-sorting (Fig. 1b). On gelation the self-sorted structures formed may interact through entanglements (Fig. 1bi)[4,5] or narcissistic self-sorting may continue, resulting in the formation of two completely independent interpenetrating gel networks (Fig. 1bii).[6] Alternatively, the two LMWGs may co-assemble into the same primary structures pre-gelation (Fig. 1c). The arrangement of the gelator molecules within the primary structures may be random[7,8] or

result in an alternating pattern of the two gelators[9,10] depending on gelator design. If the gelators exhibit some degree of self-discrimination, the resulting primary structures may contain sections that contain only one (or a higher proportion of one) gelator. This could result in preferential entanglement in
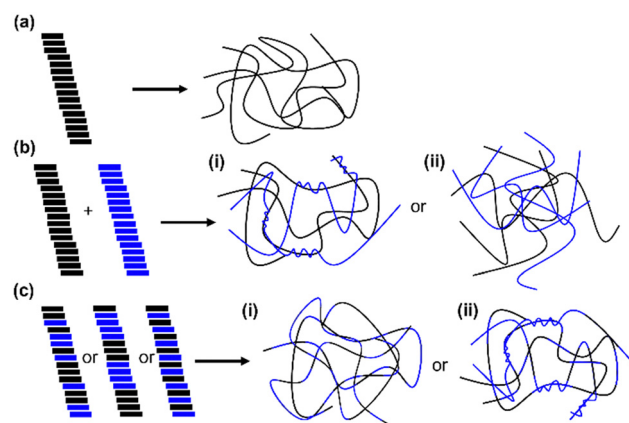

Fig. 1 (a) Cartoon showing the possible outcomes of assembly of (a) a single gelator, (b) two gelators that self-sort to individually form fibres that may (i) interact or (ii) form independent interpenetrating networks, and (c) two gelators that co-assemble into the same fibres. This can be completely random, or the components may have a slight preference for self-interaction, resulting in formation of blocks of each component, or the two components may alternate in an ordered manner. Entanglements in such networks may be (i) random or (ii) have preferential entanglement between specific sections of the primary fibres.

*[a] School of Chemistry, University of Glasgow, Glasgow, G12 8QQ, UK.
E-mail: dave.adams@glasgow.ac.uk*

[b] ISIS Pulsed Neutron and Muon Source, Harwell Science and Innovation Campus, Didcot, OX11 0QX, UK

† Electronic supplementary information (ESI) available. See DOI: https://doi.org/10.1039/d3sm00521f

specific sections of the gel network (Fig. 1cii).[11] This would change the cross-linking density and thereby the mechanical properties of the final gel.

Mixing two LMWGs allows fine control of material properties.[12–14] Sequential assembly based on the pK_a of peptide-based LMWGs has been shown to allow some predictability over the system.[15,16] Additionally, the chirality of the amino acids in peptide-based LMWGs provides a tool for changing the behaviour of these systems. Previous work has stated the importance of homochirality in allowing like-with-like intermolecular interactions that allow self-assembly of peptide-based systems and ultimately the properties of the resulting materials.[17] Homochiral systems were found to be more thermally and mechanically stable compared to their heterochiral equivalents.[17] Homochiral peptide systems formed more uniform assemblies while heterochiral systems formed self-sorted, heterogenous assemblies.[17] The Marchesan group has conducted several studies comparing homo- and heterochiral assemblies. Their work, among others, shows the advantages of heterochiral systems, such as the potential to fine-tune the behaviour of peptide-based hydrogels, such as their gelation kinetics,[18] rheological properties, protease degradation rates using the number and position of R-amino acids, and thereby their utility for biomedical applications.[19] Other work demonstrates the preference of β-sheet forming peptides for homochiral pairing over heterochiral pairing.[20] Although the (S)- and (R)-β-sheets have the same pattern of hydrogen-bond donors and acceptors, the amino acid side chains point in opposite directions. This means that the heterochiral systems will have less favourable alignment for further interactions, such as π–π stacking of aromatic groups. This was expressed as a preference for homochiral assembly and hence self-sorting in the heterochiral systems.[18] Such studies highlight the importance of considering steric effects as well as intermolecular interactions when designing peptide-based systems.[20] However, it is hard to predict how molecules are going to interact.

Here, we investigate multicomponent systems containing one of two possible stereoisomers of the well-studied peptide-based LMWG 2NapFF mixed with a variety of N-functionalised dipeptide based LMWGs (Fig. 2). Most studies focus on 2Nap-(SS)-FF.[21–27] We have included 2Nap-(RS)-FF to highlight the effect of changing chirality on these systems and show how this can be a powerful tool in tuning the properties of these systems. One diastereomer of 2NapFF is included in all the multicomponent systems to exemplify a range of possible properties accessible using multicomponent systems. From the work discussed above, one could predict that the 2Nap-(SS)-FF multicomponent systems are more likely to co-assemble, while the 2Nap-(RS)-FF multicomponent systems are more likely to self-sort since all the second components have (SS)-configuration. We also examine several different concentration ratios to investigate how the outcome of a multicomponent system can be influenced by changing the concentration ratio while maintaining the same total gelator concentration (10 mg mL^{-1}). This provides an easy method for tuning the mechanical properties of a system while keeping the same desired components.
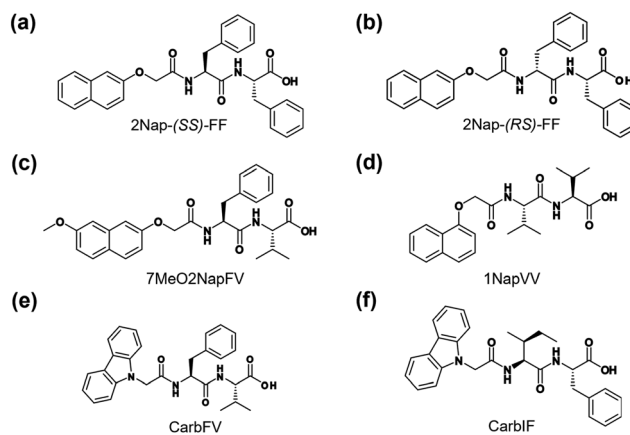

Fig. 2 Chemical structures of the components studied here: (a) 2Nap-(SS)-FF, (b) 2Nap-(RS)-FF, (c) 7MeO2NapFV, (d) 1NapVV, (e) CarbFV and (f) CarbIF.

Results and discussion

Multicomponent assembly at high pH

Stock suspensions of each component were prepared at a concentration of 10 mg mL^{-1}. These suspensions were allowed to stir overnight to ensure homogenous dispersal of the gelators. The resulting suspensions were adjusted to pH 10.5 before mixing for 2 hours with a stock suspension of the second component to give multicomponent systems with the following concentration ratios (second component:2NapFF): 7.5:2.5, 5:5 and 2.5:7.5 (mg mL^{-1}:mg mL^{-1}), to achieve a total dipeptide concentration of 10 mg mL^{-1}. The multicomponent suspensions were adjusted to pH 10.5 before use. To ensure the data for each technique was readily comparable, the same stock suspensions were used to prepare all samples for each individual technique to reduce any potential batch-to-batch variability.

7MeO2NapFV, 1NapVV and CarbFV all form non-viscous solutions that do not exhibit shear-thinning behaviour at a concentration of 10 mg mL^{-1} (Fig. 3). These components therefore do not form long, 1D structures in solution at high pH when alone.[28] When preparing multicomponent suspensions, 7MeO2NapFV and 1NapVV reduced the viscosity and shear-thinning behaviour of the system, suggesting they effectively dilute 2NapFF. We would expect this to mean that self-sorting is taking place between these components and 2NapFF in the micellar state at high pH since the 2NapFF concentration, and hence the concentration of the long 1D structures, is reduced if the second component does not co-assemble with 2NapFF. Therefore, the viscosity and shear-thinning behaviour will decrease if systems where one component (2NapFF) forms worm-like micelles while the other (7MeO2NapFV or 1NapVV) does not form worm-like micelles undergo self-sorting. However, data from other techniques is required to confirm these suggestions.

The multicomponent systems containing CarbFV show different behaviour depending on the chirality of 2NapFF (Fig. 3). When mixed with 2Nap-(SS)-FF, the resulting suspensions were
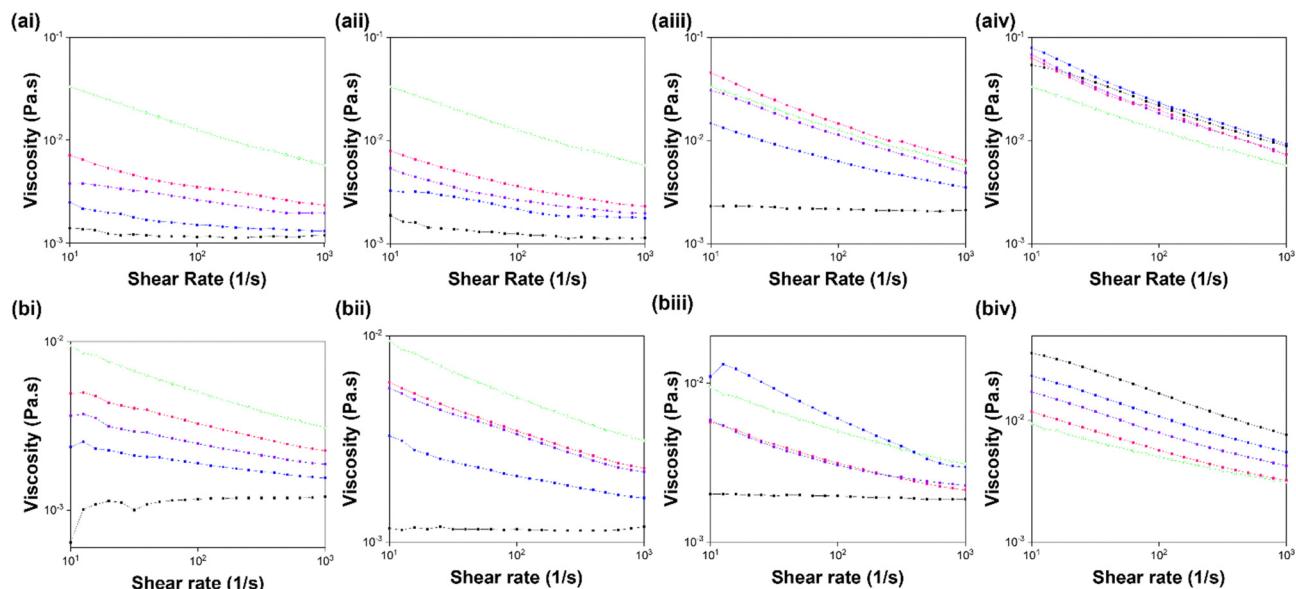
Fig. 3 Dynamic viscosity values of single and multicomponent systems of (i) 7MeO2NapFV, (ii) 1NapVV, (iii) CarbFV and (iv) CarbIF at concentration ratios second component:(a) 2Nap-(SS)-FF and (b) 2Nap-(RS)-FF: 10 mg mL^{-1}:0 mg mL^{-1} (black), 7.5 mg mL^{-1}:2.5 mg mL^{-1} (blue), 5 mg mL^{-1}:5 mg mL^{-1} (purple) and 2.5 mg mL^{-1}:7.5 mg mL^{-1} (pink). 2NapFF 10 mg mL^{-1} of the appropriate diastereomer (green) is shown in each for easy comparison. Viscosity data were collected on a single sample of each system to probe behaviour at high pH.

significantly more viscous than that of CarbFV alone. The CarbFV 5 mg mL^{-1}: 2Nap-(SS)-FF 5 mg mL^{-1} multicomponent system had similar viscosity to 2Nap-(SS)-FF (10 mg mL^{-1}). The CarbFV 2.5 mg mL^{-1}:2Nap-(SS)-FF 7.5 mg mL^{-1} suspension had greater viscosity than the 2Nap-(SS)-FF 10 mg mL^{-1} single component system. The assembly of these systems is therefore concentration dependent, suggesting the scenario is more

complicated than the suggested self-sorting observed in the 7MeO2NapFV and 1NapVV multicomponent systems.

The 2.5 mg mL^{-1}:7.5 mg mL^{-1} and 7.5 mg mL^{-1}:2.5 mg mL^{-1} CarbFV:2Nap-(RS)-FF multicomponent systems had similar viscosity values that lay between CarbFV 10 mg mL^{-1} and 2Nap-(RS)-FF and 10 mg mL^{-1}. The 5 mg mL^{-1} CarbFV:5 mg mL^{-1} 2Nap-(RS)-FF multicomponent system had even greater viscosity than
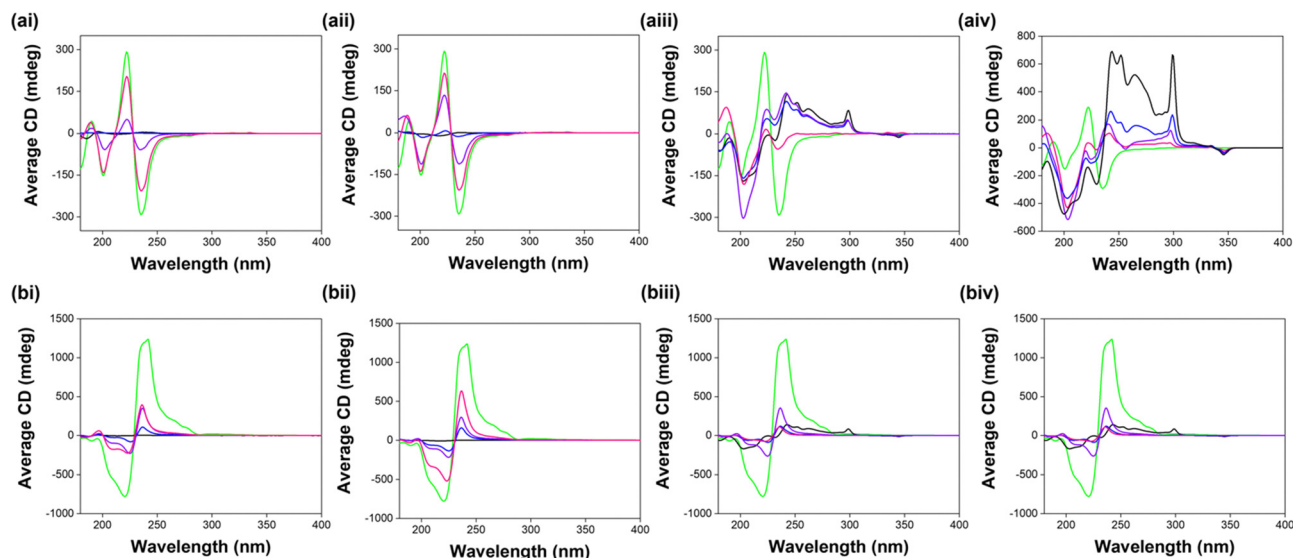

Fig. 4 CD spectra recorded from single and multicomponent systems of (i) 7MeO2NapFV, (ii) 1NapVV, (iii) CarbFV and (iv) CarbIF at concentration ratios second component: (a) 2Nap-(SS)-FF and (b) 2Nap-(RS)-FF of 10 mg mL^{-1}:0 mg mL^{-1} (black), 7.5 mg mL^{-1}:2.5 mg mL^{-1} (blue), 5 mg mL^{-1}:5 mg mL^{-1} (purple) and 2.5 mg mL^{-1}:7.5 mg mL^{-1} (pink) at pH 10.5. The CD spectrum recorded from 2NapFF 10 mg mL^{-1} of the appropriate diastereomer (green) is shown in each spectrum for easy comparison with the multicomponent systems. All data was collected in triplicate and averaged. Absorbance and HT data were recorded concurrently with the CD spectra (Fig. S1, ESI†).

2Nap-(RS)-FF 10 mg mL^{-1}. CarbIF (10 mg mL^{-1}) is the only component with greater viscosity than 2NapFF (10 mg mL^{-1}) of either chirality (Fig. 3). 2Nap-(RS)-FF appears to dilute CarbIF, indicating self-sorting. All the CarbIF:2Nap-(SS)-FF multicomponent systems have similar viscosity.

Circular dichroism (CD) was used to investigate the effect of mixing the two components on the secondary structure of the self-assemblies formed by each system. The maximum in the CD data centred at 225–230 nm stems from π–π stacking of aromatic phenylalanine residues.[29] The remaining signals most likely come from interactions between the aromatic N-terminal capping groups during self-assembly to form chiral structures.

CD data collected at high pH show that 7MeO2NapFV and 1NapVV form far fewer chiral structures or structures with less chirality than 2Nap-(SS)-FF and 2Nap-(RS)-FF, with the intensity of the peaks corresponding to 7MeO2NapFV and 1NapVV alone being far lower than any of the other systems (Fig. 4). The chirality provided by 2NapFF begins to dominate the CD spectra recorded from these multicomponent systems at even the lowest 2NapFF concentrations, with the line shapes resembling those from 2NapFF. Very little contribution from 7MeO2-NapFV or 1NapVV is observed in the multicomponent systems. 7MeO2NapFV 7.5 mg mL^{-1}:2Nap-(SS)-FF 2.5 mg mL^{-1} is the only exception (Fig. 4ai insert), where the intensity of the CD peaks is almost completely disrupted.

This suggests that 7MeO2NapFV disrupts the chirality of the structures formed when present at high enough concentrations.

This could be related to observations made during simulations performed by Isaacs et al.[30] When the concentration of one component is significantly greater than the concentration of the second component, a preference for co-assembly arises due to the increased probability of the component with the lower concentration coming into contact with the component with the higher concentration. The greatest efficiency of self-sorting always occurred when the concentrations of the two components are equal.[30] This suggests that the most efficient self-sorting takes place in the 5 mg mL^{-1}:5 mg mL^{-1} multicomponent systems. However, results from small angle neutron scattering (SANS, see below) suggest that (in 5 mg mL^{-1}: 5 mg mL^{-1} system at least) 7MeO2NapFV and 2Nap-(SS)-FF actually co-assemble. It is possible that this co-assembly is concentration dependent, and that self-sorting takes place in the 2.5 mg mL^{-1}:7.5 mg mL^{-1} system. SANS experiments on this system would be required to confirm this suggestion.

The intensity of the CD peaks increases with increasing 2NapFF concentration and never exceeds that measured from 2NapFF alone at 10 mg mL^{-1}. This suggests that the presence of 7MeO2NapFV and 1NapVV molecules perturbs the chirality of the structures formed. However, the intensity of the CD signals is enhanced compared to CD data collected from a 2Nap-(SS)-FF single component system at the same 2Nap-(SS)-FF concentration (Fig. 5), showing that the total concentration of chiral structures in the multicomponent systems is greater than in the 2Nap-(SS)-FF single component systems. This is further evidence for co-assembly.
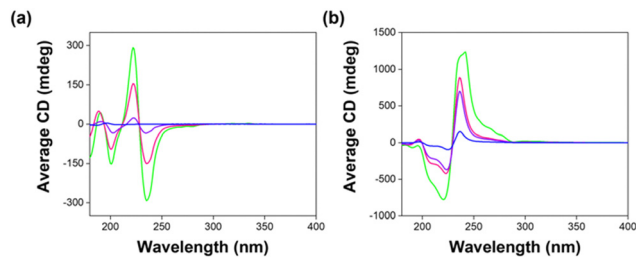

Fig. 5 CD spectra recorded from single component systems composed of (a) 2Nap-(SS)-FF and (b) 2Nap-(RS)-FF at concentrations of 10 mg mL^{-1} (green), 7.5 mg mL^{-1} (pink), 5 mg mL^{-1} (purple) and 2.5 mg mL^{-1} (blue) at pH 10.5. All data was collected in triplicate and averaged. Absorbance and HT data were recorded concurrently with the CD spectra (Fig. S2, ESI†).

We cannot completely rule out self-sorting of these systems from CD data alone as it is possible that peaks from 7MeO2-NapFV and 1NapVV are present, but they are just masked by the intense peaks measured from 2NapFF. However, if self-sorting were taking place, the CD spectrum would be the sum of the spectra from the two components individually.[6,31] This also differs from the conclusions drawn from viscosity data. The CarbFV:2Nap-(RS)-FF multicomponent systems (Fig. 4biii) shows similar behaviour to the 7MeO2NapFV and 1NapVV systems, suggesting CarbFV is undergoing co-assembly with 2Nap-(RS)-FF directing assembly. CD signals from the CarbFV 5 mg mL^{-1}:2Nap-(RS)-FF 5 mg mL^{-1} multicomponent system are more intense than those from the other two multicomponent systems, suggesting that this is the optimum concentration ratio for the co-assembly of these components. This agrees with observations from the viscosity data.

The CarbFV:2Nap-(SS)-FF multicomponent systems maintain similar CD intensity regardless of concentration ratio (apart from CarbFV 2.5 mg mL^{-1}:2Nap-(SS)-FF 7.5 mg mL^{-1}). This suggests co-assembly is taking place rather than self-sorting. The intensity and line shape of the signals are very similar to CarbFV, suggesting CarbFV is conducting assembly with 2Nap-(SS)-FF almost entirely co-assembled with CarbFV to give the same effective concentration of structures as CarbFV 10 mg mL^{-1}.

Contributions from both components are observed in the CD spectra collected from the CarbIF multicomponent systems. This indicates self-sorting, despite the behaviour reminiscent of co-assembly observed in the viscosity measurements. As the concentration of one component in the CarbIF:2NapFF multicomponent systems decreases, its contribution to the CD intensity diminishes while that of the second component increases as its concentration increases. This is further evidence for self-sorting.

The amplification of CD signals in the multicomponent systems compared to 2Nap-(SS)-FF single component systems of the same 2Nap-(SS)-FF concentration is not observed when comparing the 2Nap-(RS)-FF multicomponent systems to 2Nap-(RS)-FF single component systems. This could be due to less effective packing of (SS)-dipeptides with 2Nap-(RS)-FF compared to (SS)-dipeptides with 2Nap-(SS)-FF.

To understand the self-assembled structures in these systems, we turned to SANS. SANS data was collected from each component alone at 10 mg mL^{-1} and from 5 mg mL^{-1}: 5 mg mL^{-1} multicomponent systems. We attempted to fit each data set to all available standard cylinder models to identify the most suitable model for each. SANS data collected in the micellar phase at high pH from most of the systems studied were best fitted to a hollow cylinder model. The two exceptions were 7MeO2NapFV 10 mg mL^{-1} (fitted to an elliptical cylinder model plus a power law) and 1NapVV 10 mg mL^{-1} (fitted to a power law). The inability of 1NapVV to form cylindrical structures pre-gelation most likely due to the hydrophobicity of 1NapVV, causing it to instead form irregular aggregates.[32] More in depth discussion of the SANS data can be found in the ESI.†

The 7MeO2NapFV:2NapFF and 1NapVV:2NapFF multicomponent systems of both diastereomers of 2NapFF were fitted to a hollow cylinder model with the inclusion of a power law. The parameters obtained closely resemble those used to fit the corresponding diastereomer of 2NapFF alone at a concentration of 10 mg mL^{-1}. We therefore conclude that 7MeO2-NapFV and 1NapVV co-assemble with both diastereomers of 2NapFF. This is particularly interesting since the concentration of 2NapFF has been halved in the multicomponent systems. The inclusion of a power law in the multicomponent systems suggests increased interactions at longer length scales than in the 2NapFF single component systems (Fig. 6).

It is unclear why co-assembly between these components results in reduction in viscosity, despite maintaining the same structures formed by 2NapFF alone. We suspect that the component with the greatest susceptibility for self-assembly will control assembly. This likely comes from a multitude of factors, such as the free energy associated with the interactions

formed during self-assembly. Here, the 2NapFF diastereomers are the stronger candidates for self-assembly.

The SANS data from the CarbFV 5 mg mL^{-1}:2Nap-(SS)-FF multicomponent system were fitted to a hollow cylinder model combined with a power law with parameters similar to those obtained from fitting the CarbFV 10 mg mL^{-1} single component system. We therefore conclude that CarbFV undergoes co-assembly with 2Nap-(SS)-FF to form structures similar to those formed by CarbFV at the same total gelator concentration.

The occurrence of CarbFV-directed co-assembly suggests that the structures formed by CarbFV are more stable than those formed by 2Nap-(SS)-FF, perhaps due to more favourable interactions between CarbFV molecules than between 2Nap-(SS)-FF molecules. We do not know how the two molecules are arranged in the structures. As shown in Fig. 1, this could be completely random, or the two components may form blocks within the co-assembled structures.

We attempted to fit the CarbIF 5 mg mL^{-1}:2Nap-(SS)-FF 5 mg mL^{-1} SANS data to a vast range of single and combined cylinder models. Fitting the SANS data from the CarbIF 5 mg mL^{-1}:2Nap-(SS)-FF 5 mg mL^{-1} multicomponent system to a hollow cylinder model provided the best quality fit compared to all other single cylinder models. The parameters obtained did not resemble those from either system alone. This could be mean co-assembly is taking place, resulting in the formation of new structures, or that the two components are self-sorting, and the reduced concentration is having a significant effect on the structures formed by each component. A combination of a hollow cylinder model and a flexible cylinder model gave the lowest parameter error values and one of the lowest Chi2 values (Table S4, ESI†). It could therefore be the case that CarbIF is self-sorting in the presence of 2Nap-(SS)-FF
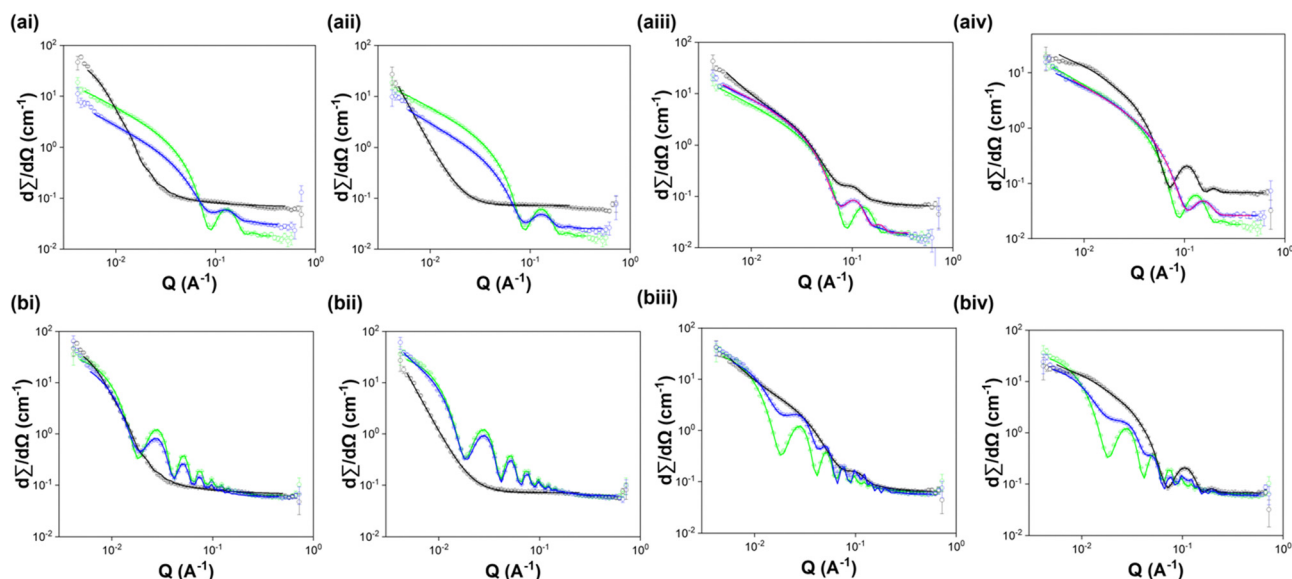

Fig. 6 Plots of SANS data (circles) and fits (solid lines) obtained from (i) 7MeO2NapFV, (ii) 1NapVV, (iii) CarbFV and (iv) CarbIF as 10 mg mL^{-1} single component systems (black) and as 5 mg mL^{-1}:5 mg mL^{-1} multicomponent systems with (a) 2Nap-(SS)-FF and (b) 2Nap-(RS)-FF (blue) at high pH. Data was also collected for both diastereomers of 2NapFF as 10 mg mL^{-1} single component systems (green) at high pH. The pink fits in aiii and aiv show the multicomponent system data when fit to a hollow cylinder + hollow cylinder combined model.

and forming flexible cylinders. Without imaging of the structures formed it is impossible to say definitively how the components are assembling in the presence of one another.

The SANS data from the CarbIF 5 mg mL⁻¹: and CarbFV 5 mg mL⁻¹:2Nap-(RS)-FF multicomponent systems only provided reasonable fits to a hollow cylinder model combined with a second hollow cylinder model (Table S5, ESI†). This is strong evidence for self-sorting. To start fitting, we input parameters from each component alone. In both cases this gave a reasonable fit. We then fit all the parameters together. The multicomponent systems only contain 5 mg mL⁻¹ of each component. We expect concentration to affect the structures formed and may result in different primary structures being formed.

The CD data from the CarbFV 5 mg mL⁻¹:2Nap-(RS)-FF 5 mg mL⁻¹ multicomponent systems suggest co-assembly is taking place. However, we were unable to obtain reasonable fits when fitting the CarbFV 5 mg mL⁻¹:2Nap-(RS)-FF 5 mg mL⁻¹ SANS data to a single hollow cylinder model. The CD signals from CarbFV may be completely masked by those from 2Nap-(RS)-FF, making the data resemble a self-sorted system.

The results from the SANS data can be partially rationalised by considering the molecular structures of the components. 7MeO2-NapFV and 1NapVV have a naphthalene at the N-terminus, as does 2NapFF. It is easy to imagine that the naphthalene rings stacking on top of each other within the co-assembled structures. CarbFV and CarbIF have a different N-terminal group, making it more difficult for these components to effectively co-assembly with 2NapFF. It is therefore preferable for them to self-sort. However, this does not explain the suspected co-assembly between CarbFV and 2Nap-(SS)-FF.

Multicomponent assembly during gelation

Molecular assembly going from high pH to low pH was probed using ¹H NMR spectroscopy. At high pH, most of the dipeptides studied are visible by ¹H NMR spectroscopy, apart from 2Nap-(RS)-FF and CarbIF. As the pH is reduced on addition of glucono-δ-lactone (GdL), the chosen trigger for gelation which results in a slow pH decrease,[31] self-assembly of the dipeptides into fibrous structures causes them to become NMR invisible.[15] We can therefore correlate the disappearance of peaks from the NMR spectrum to the percentage of the corresponding dipeptide that is self-assembled into solid-like fibres.

The percentage free molecule from the NMR data can be compared to pH data collected during gelation. Assembly begins just below the pK_a value. The NMR data matches with the plateaus in the pH data which corresponds to the pK_a values of the components.[16]

In all cases, peaks from both components start to disappear at the same pH. This suggests that the pK_a values of each component are too close for effective self-sorting via slow pH change as previously described in ref. 16. The components will therefore be assembling at the same time as each other. How the assembly of each component will be affected by concurrent assembly of the other is hard to determine. CarbFV, CarbIF and 2NapFF all disappear rapidly (Fig. 7). 7MeO2NapFV and 1NapVV assemble more slowly. 7MeO2NapFV assembles more slowly in the presence of 2NapFF, showing that the presence of a second component is altering the self-assembly. However, none of these observations confirm that co-assembly is taking place. The CarbIF integrals in all experiments were too small to measure.
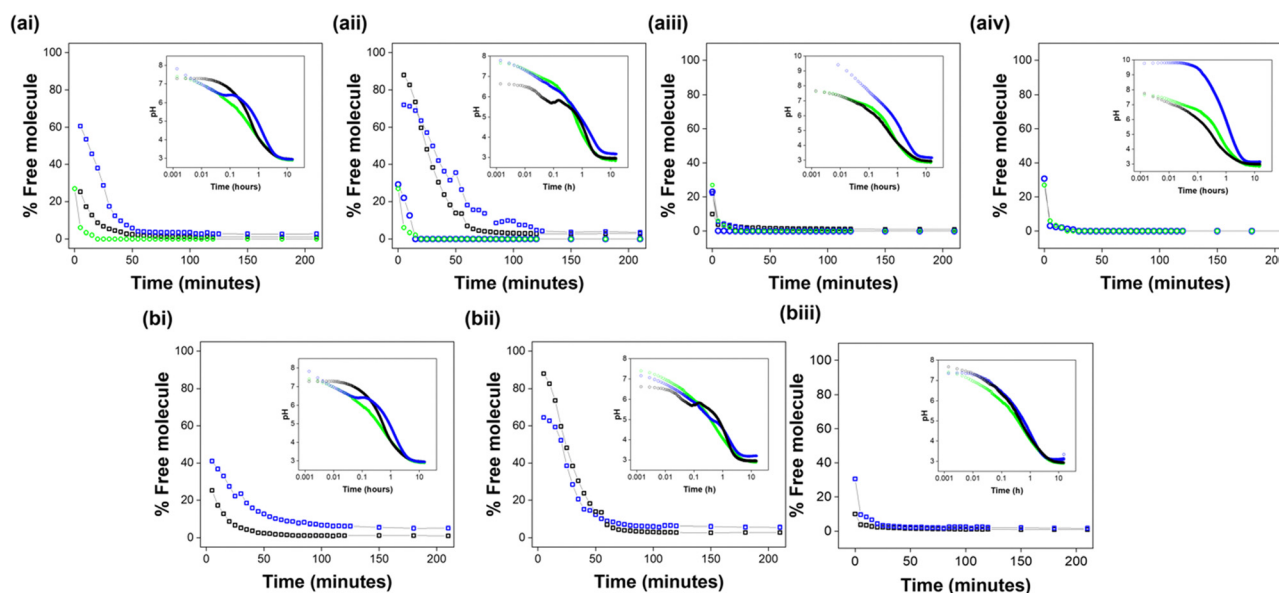

Fig. 7 Results from kinetic ¹H NMR spectroscopy experiments and measurements of pH with time (inserts) during gelation using GdL as a trigger for (i) 7MeO2NapFV, (ii) 1NapVV, (iii) CarbFV and (iv) CarbIF as 10 mg mL⁻¹ single component systems (black) and as 5 mg mL⁻¹:5 mg mL⁻¹ multicomponent systems (a) 2Nap-(SS)-FF and (b) 2Nap-(RS)-FF (blue). Data was also collected for both diastereomers of 2NapFF at a concentration of 10 mg mL⁻¹ (green).

In a similar study investigating the multicomponent assembly of a series of dipeptides functionalised with *N*-terminal naphthalene derivatives, signals from the ^{1}H NMR spectra initially disappeared at similar rates.[15] At longer times, 2NapFF disappears more quickly. This implies that co-assembly isn't uniform throughout the process. The rates of assembly of both components in each system are similar but 2NapFF does not need as much time to be fully assembled.

The integrals corresponding to 2Nap-(*RS*)-FF were too small to be measured. Since we could not measure 2Nap-(*RS*)-FF, we only have the differences between the single and multicomponent systems to rely on. For the same reason, we were also unable to measure CarbIF so this data was not included. This made probing assembly in the CarbIF:2Nap-(*RS*)-FF systems impossible. Assembly will be affected by concentration of component. It would therefore be helpful to have NMR kinetics data of the single component systems at 5 mg mL^{-1} in addition to 10 mg mL^{-1} in case this is having an effect.

Multicomponent assembly at low pH

Gels were prepared from each single and multicomponent system using GdL as a trigger. We selected GdL as a gelation trigger in favour of other possible methods, such as application of a heat–cool cycle, because the slow hydrolysis of GdL to release protons allows a uniform reduction in pH throughout the sample, resulting in formation of homogenous and reproducible gels.[33] The ability of GdL to trigger gelation of all the single and multicomponent systems studied was also important as allowed us to compare the properties of all systems in the gel state, providing greater insight into how multicomponent assembly changed the gelling behaviour of the chosen components.

Suspensions were prepared as described in the experimental methods (ESI†). Each gel was prepared by pipetting 2 mL of the required suspension into a 7 mL Sterilin vial containing preweighed solid GdL (16 mg mL^{-1}). The sample was swirled briefly by hand to dissolve the GdL. The samples were then left undisturbed for a minimum of 16 hours to allow gel formation before analysis. The final pH of all gels was between 3.2 and 3.5.

CD spectra at low pH show less obvious trends than those at high pH. The HT values measured concurrently with CD data are very high (Fig. S7, ESI†). We therefore need to be cautious about the conclusions we draw from this data. The data collected from 2Nap-(*SS*)-FF and 2Nap-(*RS*)-FF follows the opposite trend to expected with CD signal increasing with decreasing concentration (Fig. S5, ESI†). This makes data complicated to rationalise.

Again, we used SANS to probe the primary structures formed by each system at low pH. A more in-depth discussion of the SANS data can be found in the ESI.†

Since 2Nap-(*SS*)-FF directs the assembly of the 7MeO2NapFV 5 mg mL^{-1}:2Nap-(*SS*)-FF 5 mg mL^{-1} multicomponent system at high pH, it would be reasonable to expect that 2Nap-(*SS*)-FF would also direct assembly at low pH. However, the parameters obtained from fitting the SANS data collected from these systems do not match either component alone. Since the models used contain only a single cylinder model, we expect that co-assembly is maintained going from high pH to low pH. This agrees with the changes to the kinetics of gelation seen earlier when comparing the assembly of the single and multicomponent systems. However, co-assembly at low pH results in considerable changes to the primary structures that constitute the gel networks in the multicomponent system compared to the single component systems.
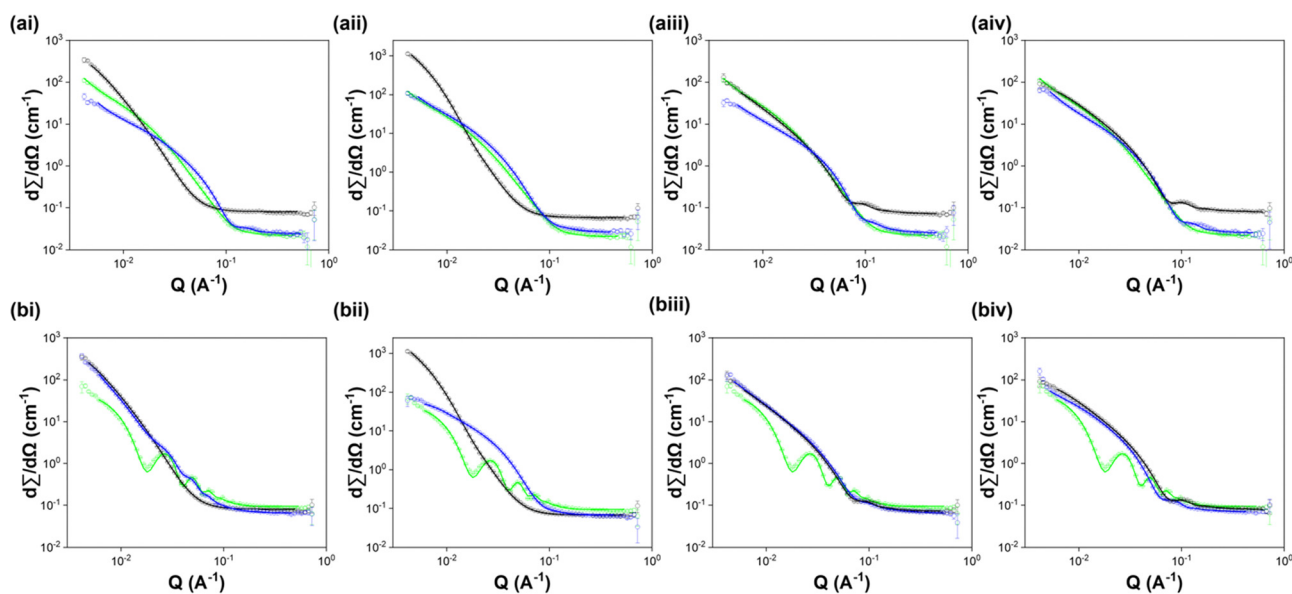

Fig. 8 Plots of SANS data (circles) and fits (solid lines) obtained from (i) 7MeO2NapFV, (ii) 1NapVV, (iii) CarbFV and (iv) CarbIF as 10 mg mL^{-1} single component systems (black) and as 5 mg mL^{-1}:5 mg mL^{-1} multicomponent systems with (a) 2Nap-(*SS*)-FF and (b) 2Nap-(*RS*)-FF (blue) in the gel state at low pH. Data was also collected for both diastereomers of 2NapFF as 10 mg mL^{-1} single component systems (green) at low pH.

The 1NapVV 5 mg mL^{-1}:2Nap-(SS)-FF 5 mg mL^{-1} and 7MeO2NapFV 5 mg mL^{-1}:2Nap-(RS)-FF 5 mg mL^{-1} multicomponent appear to continue 2NapFF directed co-assembly at low pH (Tables S6 and S7 respectively, ESI†). The 1NapVV 5 mg mL^{-1}:2Nap-(RS)-FF 5 mg mL^{-1} multicomponent system appears to transition from 2Nap-(RS)-FF directed co-assembly at high pH to 1NapVV directed co-assembly at low pH (Table S7, ESI†) (Fig. 8).

The SANS data from the CarbFV and CarbIF multicomponent systems with both diastereomers of 2NapFF were fitted to single cylinder models since combining two cylinders did not provide reasonable parameters. This suggests all these systems undergo co-assembly at low pH. This is particularly interesting since most of them are transitioning from self-sorting at high pH to co-assembly at low pH.

All these data show the effect of the identity of the second gelling component as well as the chirality of the first gelling component. While previous work highlighting the preference for homochiral interactions[20] would suggest the 2Nap-(SS)-FF multicomponent systems would be more likely to undergo co-assembly and the 2Nap-(RS)-FF multicomponent systems would undergo self-sorting, we think something else is at play in these systems.

Co-assembly in the gel phase is further suggested by powder X-ray diffraction (PXRD), although we highlight that we have concerns here over potential drying artefacts. For example, 1NapVV alone clearly crystallises on drying with numerous sharp peaks being present. When combined with either of the 2NapFF (SS or RS), only broad peaks indicative of amorphous structures are present (Fig. S21, ESI†). This suggests that co-assembly has occurred reducing the potential of the 1NapVV to crystallise on drying.

We investigated the mechanical properties of the gels formed from of all the single and multicomponent systems

using rheology. A comparison to the same diastereomer of 2NapFF as is in the multicomponent systems is included in each graph for easy comparison. The rheological data clearly shows the importance of concentration ratio in determining the mechanical properties of the final gel. The relative concentration of components therefore provides an important tool for tuning the properties of a given multicomponent gel. This agrees with previous studies showing the wide range of mechanical responses achievable by varying the concentration ratio of the components in two-gelator systems.[34–36] That said, the effect of concentration on mechanical properties does not follow an obvious trend, making it difficult to predict the outcome of altering concentration ratio.

It would be reasonable to expect that the self-sorted multicomponent systems with primary structures that closely resemble one of the components to have rheological properties that also resemble that component. However, length scales investigated using SANS do not take into account the interactions that take place at longer length scales within the gel network, for example entanglements and cross-links between individual structures. It is therefore important to be cautious when relating the results from rheological measurements to the primary structures observed using SANS.

The data shown in Fig. 9 and Fig. 10 exemplifies the vast range of rheological outcomes of preparing multicomponent systems using different components and different concentration ratios of the same two components. It can clearly be seen that preparation of two-component systems provides ample opportunity for tuning the mechanical properties of the chosen system. As can be seen from the SANS data, it is hard to predict the outcome of such mixtures, making us reliant on trial and error rather than strict design rules.

In some cases, for example 7MeO2NapFV:2Nap-(RS)-FF, varying concentration ratios allows us to obtain G' and G''
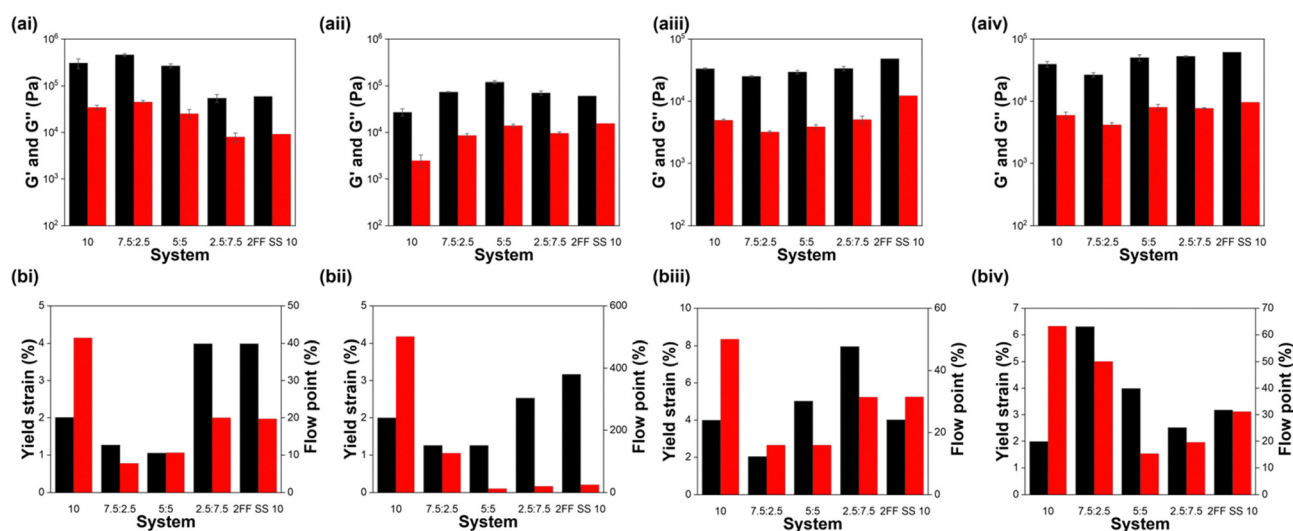

Fig. 9 (a) Average G' (black) and G'' (red) values and (b) yield strain (black) and flow point (red) values for (i) 7MeO2NapFV, (ii) 1NapVV, (iii) CarbFV and (iv) CarbIF as single component (10 mg mL^{-1}) and multicomponent systems with 2Nap-(SS)-FF of the concentration ratios defined on the x-axis. Moduli were calculated from frequency sweeps using the values for the moduli at a frequency of 10 rad s^{-1}. Error bars show the standard deviation between samples. Yield strain and flow point values were calculated from strain sweeps. All full rheology data can be found in the ESI† (Fig. S8).
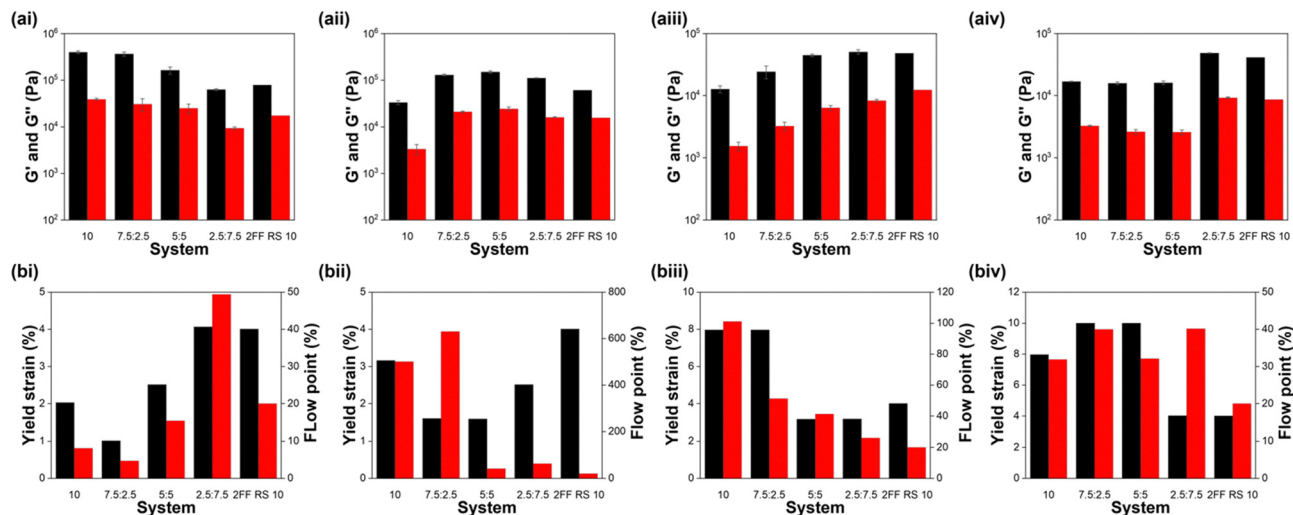
Fig. 10 (a) Average G' (black) and G'' (red) values and (b) yield strain (black) and flow point (red) values for (i) 7MeO2NapFV, (ii) 1NapVV, (iii) CarbFV and (iv) CarbIF as single component (10 mg mL^{-1}) and multicomponent systems with 2Nap-(RS)-FF of the concentration ratios defined on the x-axis. Moduli were calculated from frequency sweeps using the values for the moduli at a frequency of 10 rad s^{-1}. Error bars show the standard deviation between samples. Yield strain and flow point values were calculated from strain sweeps. All full rheology data can be found in the ESI† (Fig. S9).

values similar to the component with the highest concentration and intermediate values at a 1:1 ratio. In other cases, for example 1NapVV:2Nap-(SS)-FF and 1NapVV:2Nap-(RS)-FF, a maximum in moduli values is reached at a particular concentration ratio.

The effect of multicomponent assembly on yield stress and flow point is more complicated and does not show any clear concentration dependent trends. In-depth discussion of the trends of each set of systems can be found in the ESI.†

Conclusions

This work highlights the importance of considering the concentration ratio of components when preparing multicomponent systems. A range of mechanical properties can be accessed from a single two-gelator system by varying the concentration ratio. This allows preparation of a system from two essential components that also has the desired mechanical properties. While the ideal situation is to be able to design a system with predetermined properties, we have shown the importance of testing a variety of conditions.

Our results show that preparing multicomponent systems using two components with different N-terminal capping group does not guarantee self-sorting, as was seen with the CarbFV:2NapFF systems. The identity and order of amino acids in the peptide chain clearly also plays a role in determining how the two components in the system assemble in the presence of one another and thereby the properties of the resulting system. We suspect that the gelator with the most favourable interactions directs co-assembly. While the techniques used here provide evidence for self-sorting or co-assembly at the molecular and fibre levels of self-assembly, we cannot draw conclusions about interactions between the two components at the gel network level.

We have shown how altering the chirality of a single amino acid residue in one of the components can greatly increase the variety of structures and therefore properties available to two-component gelator–gelator systems. It is interesting that, despite previous work demonstrating a preference for homochiral assembly in peptide-based multicomponent supramolecular systems, no significant disruption to assembly was observed in the 2Nap-(RS)-FF multicomponent systems and in some cases, these systems had enhanced mechanical properties compared to their 2Nap-(SS)-FF counterparts. There was also no change from co-assembly to self-sorting when 2Nap-(SS)-FF was replaced with 2Nap-(RS)-FF. This suggests that the propensity for 2NapFF of either chirality to self-assemble into ordered structures outweighs any preference for homochiral assembly in the systems studied.

We expect that the component with the greatest propensity for self-assembly will direct co-assembly. For example, CarbFV appears to have stronger self-assembly at high pH than 2Nap-(SS)-FF, based on CD data. Co-assembly of these two components with 2Nap-(SS)-FF therefore results in formation of structures that more closely resemble CarbFV and CarbIF. When two components have similar abilities to self-assemble, for example CarbIF and 2Nap-(RS)-FF, self-sorting is more likely to take place.

Author contributions

Conceptualization: LM, DA; methodology: LM, RG, JD, ED, DA; validation: LM, SB; formal analysis: LM, SB; investigation: LM, SB, RG, JD, ED, DA; data Curation: LM; writing – original Draft: LM; writing – review & editing: all; visualisation: LM; supervision: ED, DA; project administration: DA; funding acquisition: ED, DA.

Conflicts of interest

There are no conflicts to declare.

Acknowledgements

Notes and references

1 F. Sheehan, D. Sementa, A. Jain, M. Kumar, M. Tayarani-Najjaran, D. Kroiss and R. V. Ulijn, *Chem. Rev.*, 2021, **121**, 13869–13914.

2 R. V. Ulijn and A. M. Smith, *Chem. Soc. Rev.*, 2008, **37**, 664–675.

3 X. Du, J. Zhou, J. Shi and B. Xu, *Chem. Rev.*, 2015, **115**, 13165–13307.

4 B. O. Okesola, Y. Wu, B. Derkus, S. Gani, D. Wu, D. Knani, D. K. Smith, D. J. Adams and A. Mata, *Chem. Mater.*, 2019, **31**, 7883–7897.

5 A. M. Brizard, M. C. A. Stuart and J. H. van Esch, *Faraday Discuss.*, 2009, **143**, 345–357.

6 H. Shigemitsu, T. Fujisaku, W. Tanaka, R. Kubota, S. Minami, K. Urayama and I. Hamachi, *Nat. Nanotechnol.*, 2018, **13**, 165–172.

7 L. N. J. de Windt, C. Kulkarni, H. M. M. ten Eikelder, A. J. Markvoort, E. W. Meijer and A. R. A. Palmans, *Macromolecules*, 2019, **52**, 7430–7438.

8 M. Zhou, A. M. Smith, A. K. Das, N. W. Hodson, R. F. Collins, R. V. Ulijn and J. E. Gough, *Biomaterials*, 2009, **30**, 2523–2530.

9 A. Das and S. Ghosh, *Chem. Commun.*, 2011, **47**, 8922–8924.

10 N. S. S. Kumar, M. D. Gujrati and J. N. Wilson, *Chem. Commun.*, 2010, **46**, 5464–5466.

11 N. Singh, A. Lopez-Acosta, G. J. M. Formon and T. M. Hermans, *J. Am. Chem. Soc.*, 2022, **144**, 410–415.

12 L. E. Buerkle and S. J. Rowan, *Chem. Soc. Rev.*, 2012, **41**, 6089–6102.

13 E. V. Alakpa, V. Jayawarna, A. Lampel, K. V. Burgess, C. C. West, S. C. J. Bakker, S. Roy, N. Javid, S. Fleming, D. A. Lamprou, J. Yang, A. Miller, A. J. Urquhart, P. W. J. M. Frederix, N. T. Hunt, B. Peault, R. V. Ulijn and M. J. Dalby, *Chem*, 2016, **1**, 298–319.

14 S. Fleming and R. V. Ulijn, *Chem. Soc. Rev.*, 2014, **43**, 8150–8177.

15 C. Colquhoun, E. R. Draper, E. G. Eden, B. N. Cattoz, K. L. Morris, L. Chen, T. O. McDonald, A. E. Terry, P. C. Griffiths, L. C. Serpell and D. J. Adams, *Nanoscale*, 2014, **6**, 13719–13725.

16 K. L. Morris, L. Chen, J. Raeburn, O. R. Sellick, P. Cotanda, A. Paul, P. C. Griffiths, S. M. King, R. K. O'Reilly, L. C. Serpell and D. J. Adams, *Nat. Commun.*, 2013, **4**, 1480.

17 S. Basak, I. Singh, A. Ferranco, J. Syed and H.-B. Kraatz, *Angew. Chem., Int. Ed.*, 2017, **56**, 13288–13292.

18 O. Bellotto, S. Kralj, R. De Zorzi, S. Geremia and S. Marchesan, *Soft Matter*, 2020, **16**, 10151–10157.

19 S. Marchesan, K. E. Styan, C. D. Easton, L. Waddington and A. V. Vargiu, *J. Mater. Chem. B*, 2015, **3**, 8123–8132.

20 D. M. Chung and J. S. Nowick, *J. Am. Chem. Soc.*, 2004, **126**, 3062–3063.

21 C. Colquhoun, E. R. Draper, R. Schweins, M. Marcello, D. Vadukul, L. C. Serpell and D. J. Adams, *Soft Matter*, 2017, **13**, 1914–1919.

22 K. McAulay, P. A. Ucha, H. Wang, A. M. Fuentes-Caparros, L. Thomson, O. Maklad, N. Khunti, N. Cowieson, M. Wallace, H. Cui, R. J. Poole, A. Seddon and D. J. Adams, *Chem. Commun.*, 2020, **56**, 4094–4097.

23 E. R. Draper, H. Su, C. Brasnett, R. J. Poole, S. Rogers, H. Cui, A. Sneddon and D. J. Adams, *Angew. Chem.*, 2017, **129**, 10603–10606.

24 A. Z. Cardoso, L. E. Mears, B. N. Cattoz, P. C. Griffiths, R. Schweins and D. J. Adams, *Soft Matter*, 2016, **12**, 3612–3621.

25 L. Thomson, R. Schweins, E. R. Draper and D. J. Adams, *Macromol. Rapid Commun.*, 2020, e2000093.

26 D. Giuri, L. J. Marshall, B. Dietrich, D. McDowall, L. Thomson, J. Y. Newton, C. Wilson, R. Schweins and D. J. Adams, *Chem. Sci.*, 2021, **12**, 9720–9725.

27 F. Avino, A. B. Matheson, D. J. Adams and P. S. Clegg, *Org. Biomol. Chem.*, 2017, **15**, 6342–6348.

28 P. Terech and R. G. Weiss, *Chem. Rev.*, 1997, **8**, 3133–3160.

29 S. Marchesan, C. D. Easton, F. Kushaki, L. Waddington and P. G. Hartley, *Chem. Commun.*, 2012, **48**, 2195–2197.

30 A. X. Wu and L. Isaacs, *J. Am. Chem. Soc.*, 2003, **125**, 4831–4835.

31 K. Sugiyasu, S. I. Kawano, N. Fujita and S. Shinkai, *Chem. Mater.*, 2008, **20**, 2863–2865.

32 L. Chen, T. O. McDonald and D. J. Adams, *RSC Adv.*, 2013, **3**, 8714–8720.

33 D. J. Adams, M. F. Butler, W. J. Frith, M. Kirkland, L. Mullen and P. Sanderson, *Soft Matter*, 2009, **5**, 1856–1862.

34 E. Rosa, E. Gallo, T. Sibillano, C. Giannini, S. Rizzuti, E. Gianolio, P. L. Scognamiglio, G. Morelli, A. Accardo and C. Diaferia, *Gels*, 2022, **8**, 831.

35 M. Halperin-Sternfeld, M. Ghosh, R. Sevostianov, I. Grigoriants and L. Adler-Abramovich, *Chem. Commun.*, 2017, **53**, 9586–9589.

36 C. Diaferia, M. Ghosh, T. Sibillano, E. Gallo, M. Stornaiuolo, C. Giannini, G. Morelli, L. Adler-Abramovich and A. Accardo, *Soft Matter*, 2019, **15**, 487–496.